Modelling the effect of laser pulse duration on the 1-Dimension time-space expansion of laser produced plasmas

Huda Oda Saheb, Wissam H. Mahdi
Department of Physics, Faculty of Education for girls, University of Kufa, Najaf, Iraq
hudaoda2020@gmail.com, wisam.alajeeli@uokufa.edu.iq

Abstract
in this research, the tin (Sn) plasmas created by ND: YAG laser λ=1064 nm was simulated with 1D-hydrodynamic code (MED103) for different pulse duration in nanosecond and picosecond regime.the laser pulse duration of (1-40) ns and (1-750) ps FWHM was focused on cylindrical target with spot radius of 100 µm and fixed intensity of $1.59*10^{11}$ w/cm^2 for all pulses. The Evolution of electron temperature T_e, ion rate Z* and velocity of electrons V_e in space and time of Sn plasmas were compared between nanosecond and picosecond laser pulse duration regime.

Keywords -Sn plasmas, lithography, 1-D LPP code, extreme ultraviolet (EUV), laser-produced plasma LPPs

1.Introduction

the studies have focused on the process of nanosecond and picosecond laser ablation according to its expanding applications like lithography, three-dimensional imaging, x-ray microscopy of a living cell, and x-ray-free electron laser. The interaction of a powerful laser beam with a solid sample[1] results in a crater formation on the sample surface and the creation of laser plasma composed of excited atoms and ions of the sample[2, 3]. This plasma is of analytical interest for solid surface characterization plasma in extreme ultraviolet (EUV)[4] and X-ray spectrum. The spatial-temporal distribution of plasma parameters (SXR) region.[5]Several studies examined the morphology of surfaces after nanosecond laser ablation. For predicting the ablation depth and diameter, most of these studies only took evaporation into account. Lasers with picosecond pulse duration are of particular interest for ablation as the pulse duration is less than the typical thermalization characteristic Time of a few nanoseconds. Due to a much smaller thermal diffusion depth, high-precision ablation and minimal damage can be obtained with picosecond lasers duration.

Theory

The interaction of the nanosecond laser with the material is essentially a photo-thermal process because a nanosecond is significantly longer than the phonon-electron relaxation time. The substance will absorb extremely high power density when it is exposed to a pulsed laser. The laser energy is transformed during the procedure into heat deposition on the material's surface.[6, 7]and causes the irradiated area's temperature to rise quickly. [8, 9].This study compared nanosecond and picosecond laser ablation of Sn in the air. [10-12]The laser-induced plasma properties were determined from spectroscopic measurements[13].

1. Electron temperature variation
2. Spacetime evolution and pressure variation over time
3. ions temperature
4. ion rate Z*
5. distribution of the velocity of electrons V_e of Sn
6. The laser-matter interaction program Med103 is used to calculate the spatial and temporal hydrodynamics (improved from the MEDUSA code). Plasma hydrodynamics were modeled using

the Fortran LPP code Med103, which is an updated version of the MEDUSA code. Christiansen developed the MEDUSA code in 1974 for the UKAEA group at Culham Laboratory with the intention of simulating inertial confinement fusion.[14, 15]

2. Results and Discussion

The program MED103 used code 1-D hydrodynamic to simulate Laser produced (Sn=50) plasmas (a developed version of Medusa). The Medusa program MED103 used code 1-D hydrodynamic to simulate plasmas parameters of Laser created from the (Sn=50) metal target (Medusa was developed version cod), the laser pulse with wavelength (λ =1064 nm) (ρ) its the density of power = ($1*10^{15}$ $w.cm^{-2}$) and (FWHM) width of pulse =(10 to 40)ns Time and Time Again (1 to 750)ps, fall on the constant Target with Cylindrical geometric radius shape (100 µm). The thickness of the cylindrical target (100 µm) was, By default, 400 cells as a mesh, and the simulation time of the total process= (1 ns) with a time-step of (40 ns) and (750) ps.

2.1 The Difference Of Electron Temperature For A Nanosecond And Picosecond Laser Pulse Duration

Figure 1. (A,B, and C) shows the temporal and spatial variation of the electron temperature. Three columns of the diagrams of Figure 1. (A,B, and C) The first column (A) represents five subsets of the electron temperature with distance for five values of different laser pulses, while the second column (B) shows five subsets of the electron temperature with Time, and the last column in Figure (C) shows five three-dimensional subgraphs of the electroin temperature in space and Time.

The electrons temperature increases in Time, gradually with increasing the duration of the pulse laserduration from 33.5 eV at the laser pulse duration of (1 ns), the temperature rises to reach more than 98 eV at the pulse laser duration of (10) ns, then decreases slightly to stabilize and reaches 84.5 eV at 40 ns, and the plasma volume expands from µm (1000-6000) by varying the duration of the laser pulseThen the plasma is cooled as shown in Figure (A,B), the hottest region is near the centre of the target at the peak of the laser pulse. The region is narrow-band at a laser pulse duration of (1 ns), then it expands as the laser pulse duration increases to its highest value at 40 ns. Figure (C) indicates the temporal and spatial distribution of electrons (3D) for a different laser pulse duration.

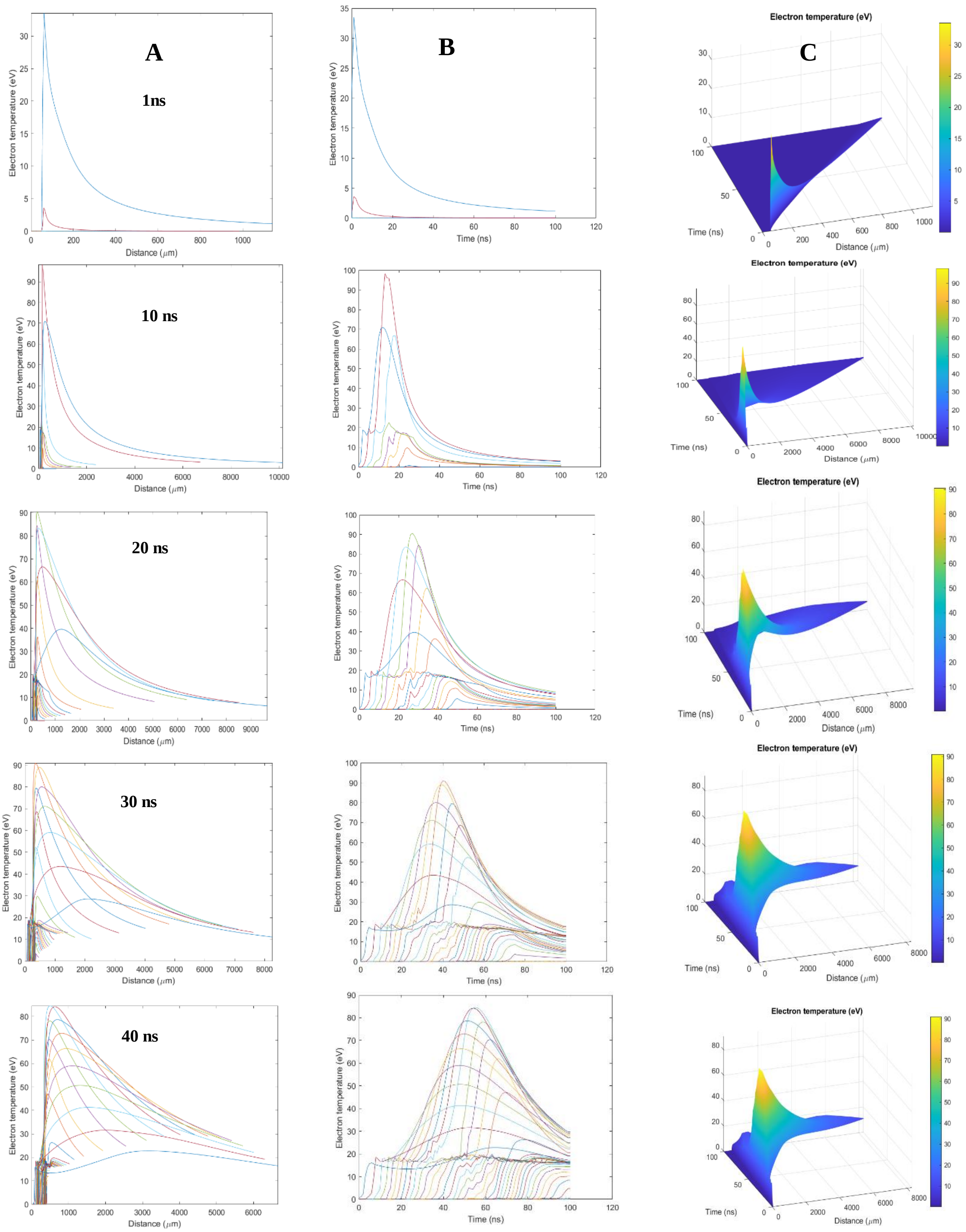

Figure 1(A,B) show Evolution of electrons temperature T_e spatially and temporally by MED103 program simulation results of tin plasma produced by Nd:YAG laser for 5different pulse duration in nanosecond (C) shows the 3D spatial and temporal distribution of the temperature of T_e electrons

The Figure(2) shows a picosecond for four values of laser pulse duration at (1,250,500,750) ps. (A,B, and C), respectively, the temperature of the electrons increases temporally, gradually increasing from 0.8 eV with laser pulse duration at 1 ps to 25 eV at 750 ps of laser pulse duration, and the plasma volume is constant,Figure (C) shows (3D) for different laser pulse duration.

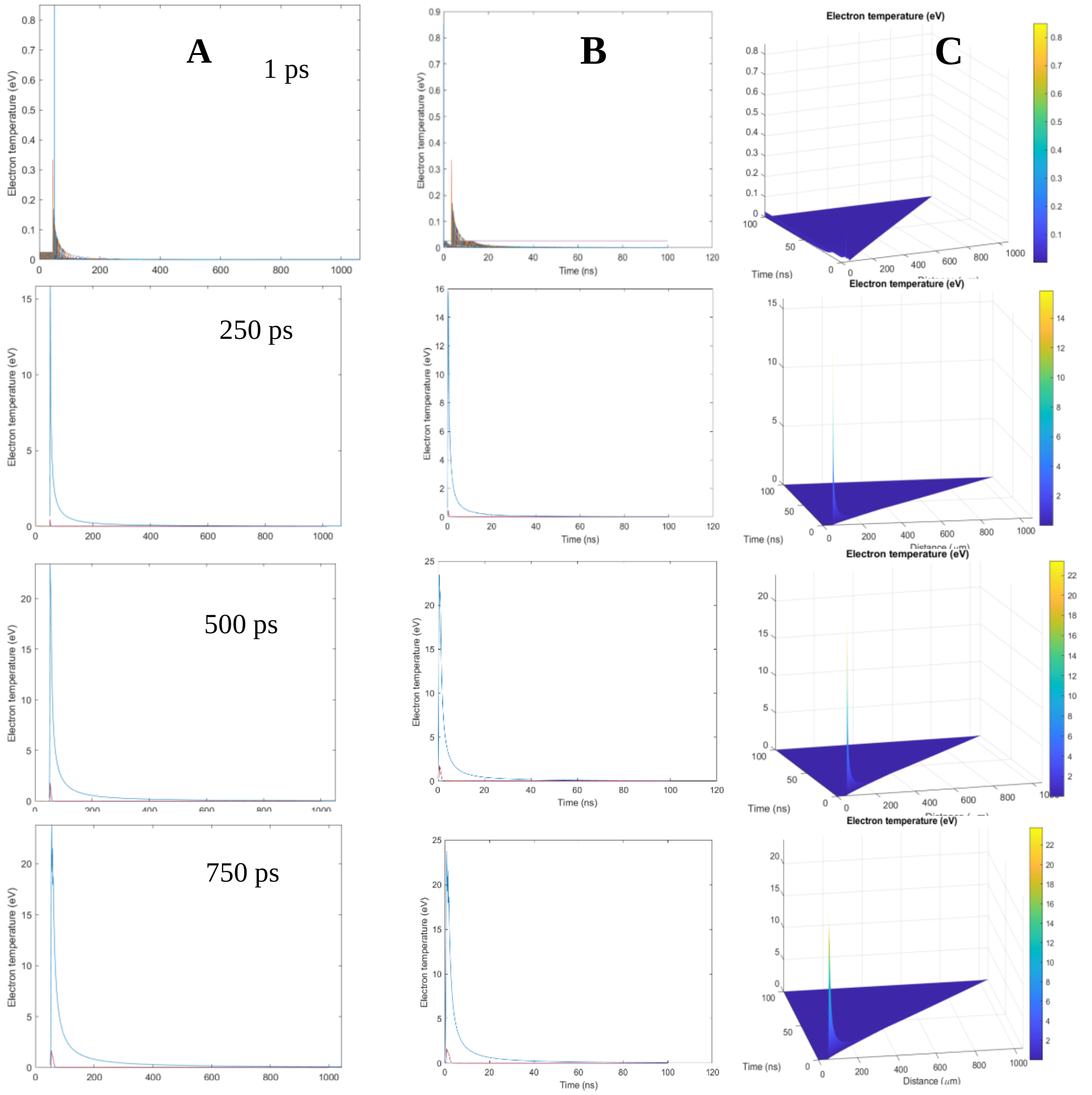

Figure 2(A, B).show picosecond laser pulse duration. Evolution of temperature of T_e electrons spatially and temporally from MED103 program simulation results of tin plasma produced by Nd:YAG laser. (C) shows the 3D spatial and temporal distribution temperature of T_e electrons

Table 1 : shows a summary of the maximum value of theelectrons temperature T_e, which we obtained from the simulation of the MED103 program for a nanosecond and picosecond laser pulse duration.

Pulse Duration	Maximam value:electrons temperature (eV)	Time ns	Distance µm
1 ps	0.84947	0.00163203	49.875
250 ps	15.872	0.401773	15.633
500 ps	23.445	0.602556	52.862
750 ps	23.798	0.903504	45.662
1ns	33.528	1.00262	61.04
10ns	98.293	13.0049	159.58
20ns	90.531	27.0067	272.19
30ns	90.947	40.0014	346.04
40 ns	84.557	55.0039	495.24

2.2 spatial and temporal ion rate Z* variation in different pulse duration

Figure 3. (A, B, and C) respectively show the beginning of the reaction, we notice that the maximum value of the ion rate Z * is (9) at the edge of the plasma, then it drops to (7) at different times and distances until the end of the laser pulse (at the edge of the plasma). Then it rises gradually with increasing the laser pulse duration to 40 ns; after that, Z* stabilizes at 21. This happens because the plasma expands very quickly. Figure 7. (C) indicates the ion rate's three-dimensional spatial and temporal distribution.

Figure 4 (A,B) shows that at the beginning of the interaction, we notice the maximum value of the ion rate Z * is (3.6) at the edge of the plasma, then it rises to reach (4.55) temporally and remains constant at (1100 µm) spatially until the end of the duration of the laser pulse (at the edge of the plasma). Figure 8c indicates the three-dimensional spatial and temporal distribution of the ion rate.

Vol 12 Issue 04 2023
ISSNNO:2230-5807

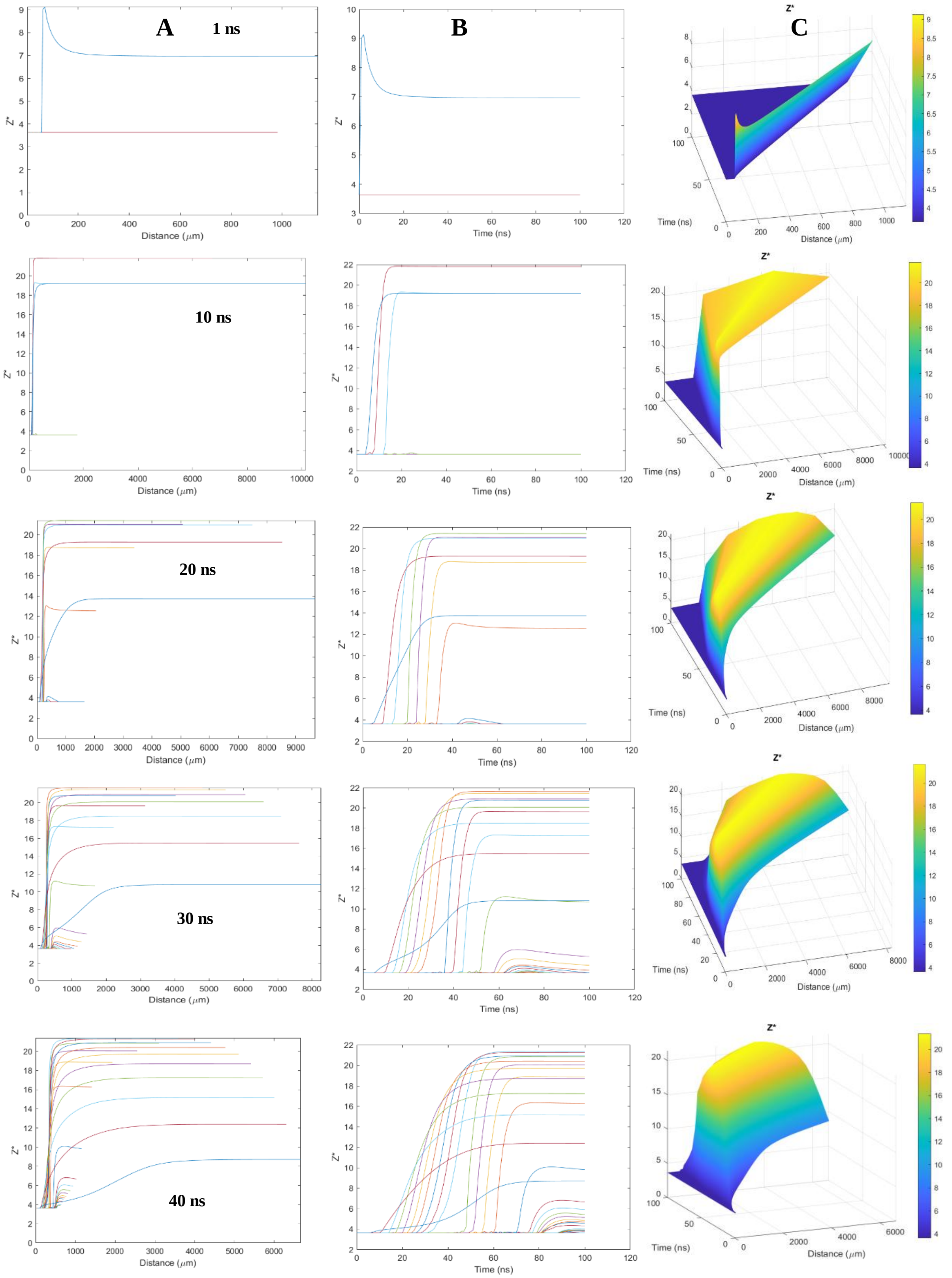

Figure (3) (A,B) Shows the evolution of value of the ion rate Z* spatially and temporally from MED103 program simulation results of tin plasma produced by Nd:YAG laser for five different pulse duration (1-40) in nanoseconds. (C) shows the 3D spatial and temporal distribution of the ion rate Z *

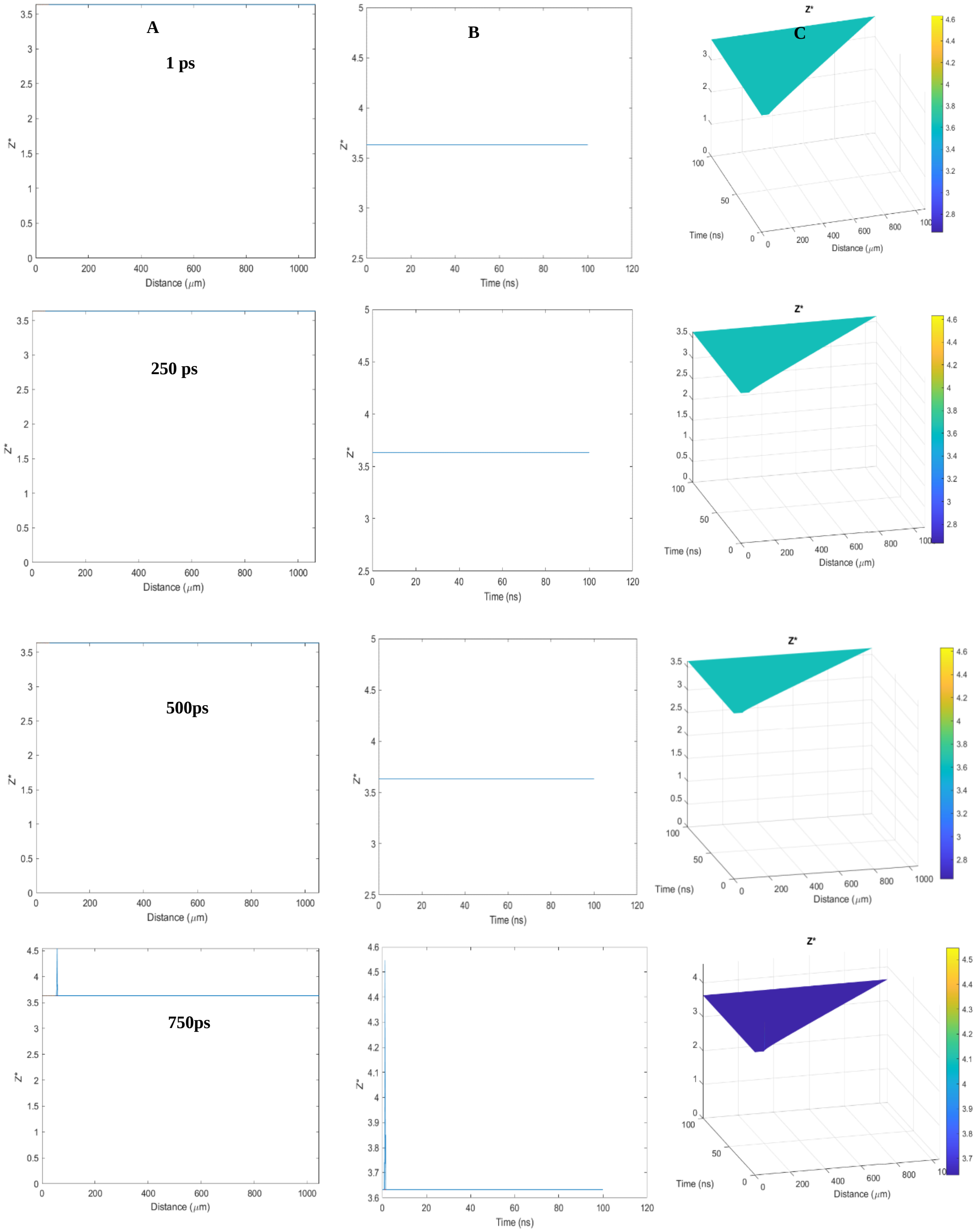

Figure (4) (A,B) Shows the evolution of the ion rate Z* spatially and temporally from MED103 program simulation results of tin plasma produced by Nd:YAG laser for four different pulse duration (1-750) in picoseconds. (C) Shows the 3D spatial and temporal distribution value of the ion rate Z *

Table 2 below: shows a summary of the ion rate Z *, which we obtained from the simulation of the MED103 program for a nanosecond and picosecond laser pulse duration from tin plasma.

Pulse Duration	Maximam value: Z*	Time ns	Distance µm
1 ps	3.6326	99.1242	1060.5
250 ps	3.6326	99.5054	1062.9
500 ps	3.6326	99.8057	1051.9
750 ps	4.5467	1.30177	57.058
1ns	33.528	9.1353	68.387
10ns	98.293	21.787	228.49
20ns	90.531	21.363	500.80
30ns	90.947	21.646	988.33
40 ns	84.557	21.319	744.96

2.3 The effect of the laser pulse duration for nanosecond and picosecond on the spatial and temporal distribution of the velocity of electrons V_e in the plasma

When the pulse duration isa nanosecond, The speed of the electrons increases spatially-temporally, starting from zero and then increasing when the plasma is formed to become 12×10^5 cm.sec^{-1} with the increase in the laser pulse duration; although the plasma expands from 1000 µm of laser pulse duration 1 ns to 7000 µm of laser pulse duration 40 ns the. Considering that the kinetic energy of electrons and ions will increase, as a result of the increase in the target temperature, which leads to an increase in the expansion velocity at the plasma edge,Figure 9. (A, B, and C) shows the Evolution of the electron velocity, Ve, spatially-temporally and in (3D) respectively produced from the laser pulse duration of a nanosecond.

At picosecond, the speed of electrons increases spatially and temporally, starting from zero and then increasing when plasma is formed to become 10×10^5 cm.sec^{-1},And the expansion of the plasma within 100 ns remains constant at 1000 µm at all the duration of the laser pulses, taking into account that the kinetic energy of the electrons and ions will increase, as a result of the high temperature of the target, which led to an increase in the expansion speed at the edge of the plasma.Figure 10. (A, B, and C) shows the Evolution of the electron velocity, Ve, spatially-temporally and in (3D), respectively produced from the laser pulse duration ofa picosecond.

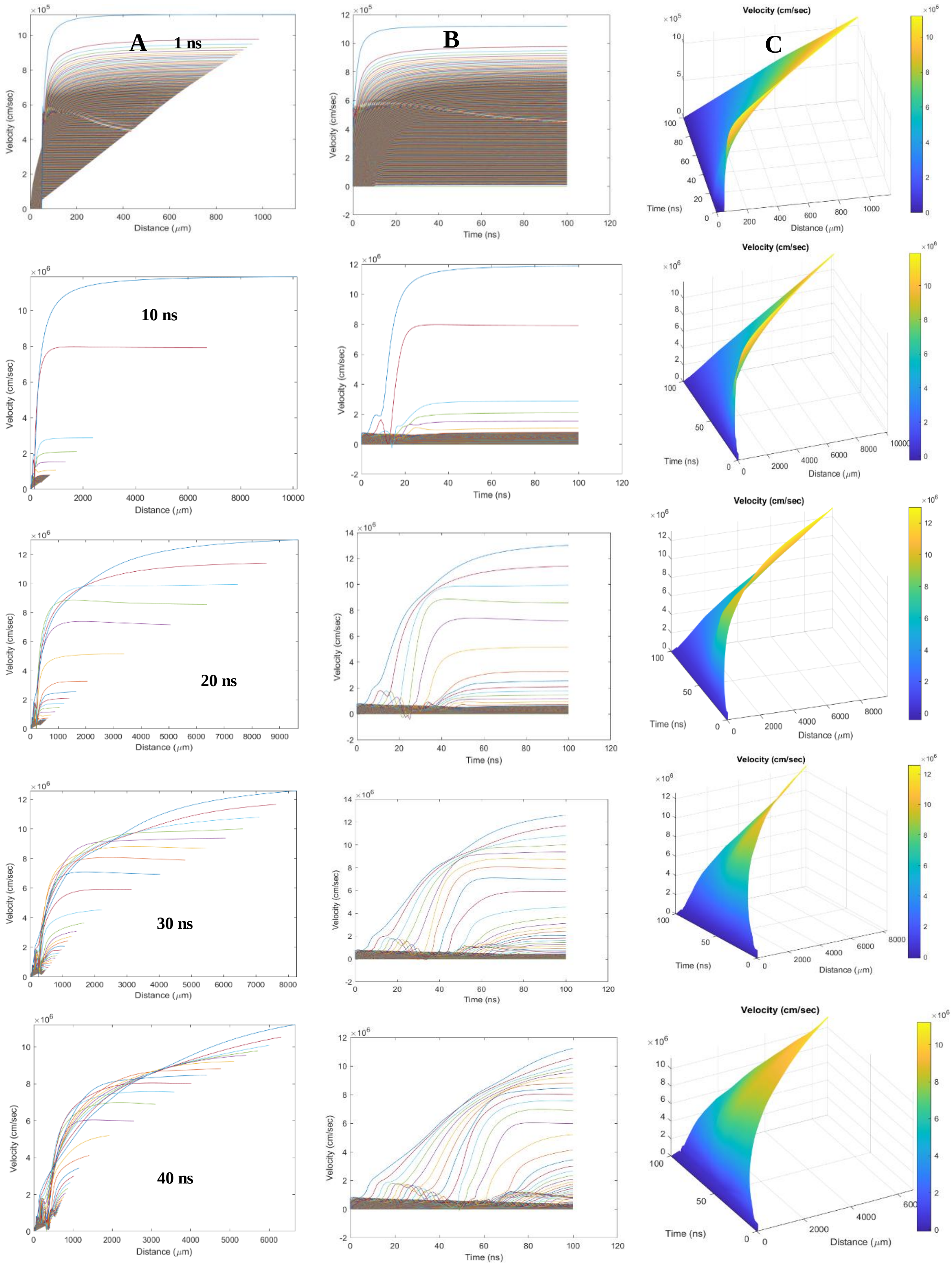

Figure (5) (A,B)Shows the evolution ofVelocity spatially and temporally from MED103 program simulation results of tin plasma produced by Nd:YAG laser for five different pulse duration (1-40) in nanoseconds. (C) shows the 3D spatial and temporal distribution of the value Velocity

Vol 12 Issue 04 2023
ISSNNO:2230-5807

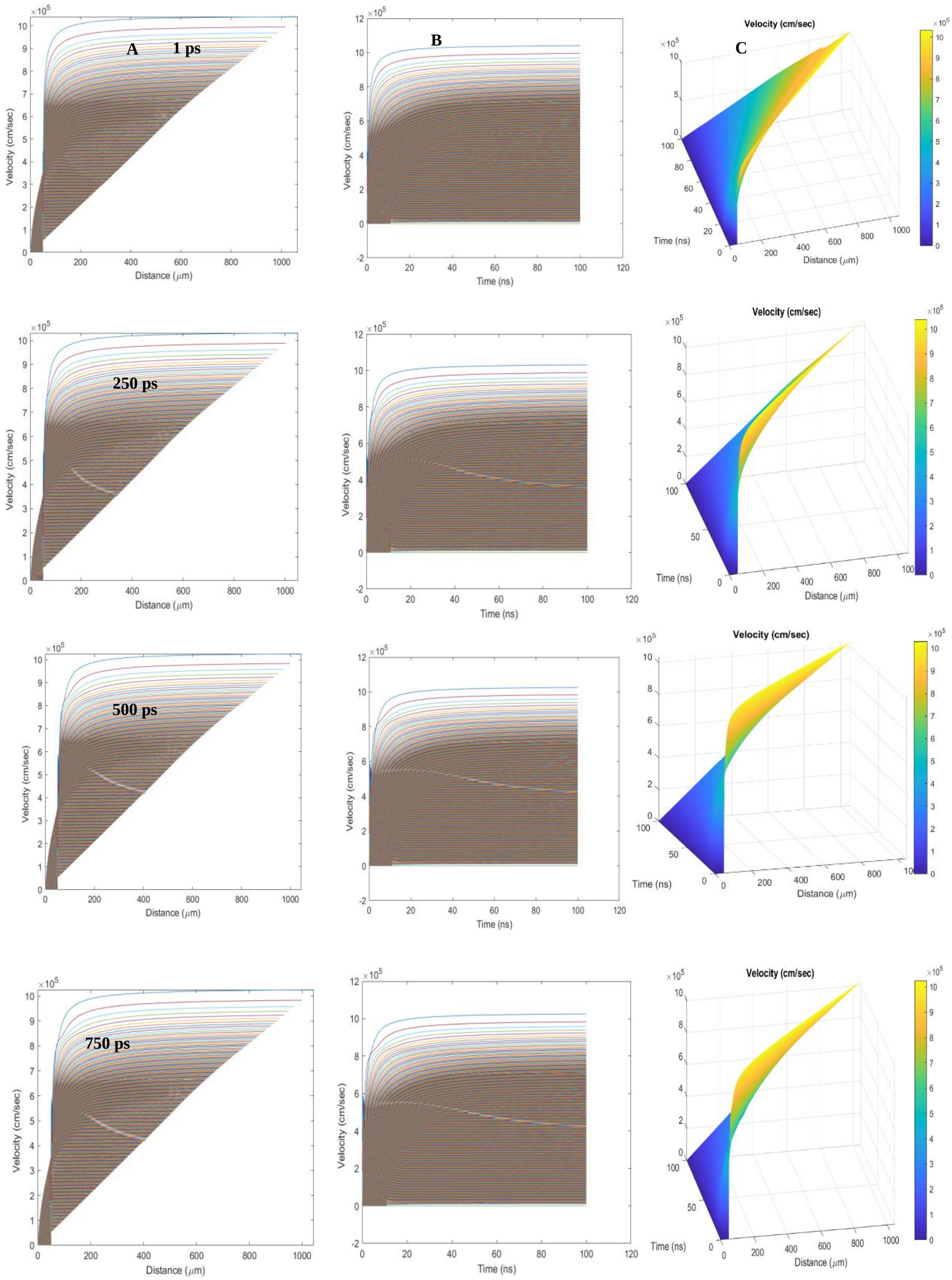

Figure (6) (A,B) Shows the evolutionof Velocity spatially and temporally from MED103 program simulation results of tin plasma produced by Nd:YAG laser for four different pulse duration (1-750) in picoseconds. (C) shows the 3D spatial and temporal distribution of the Velocity

Table 3: shows a summary of the Evolution of velocity ofV_e in the tin plasma spatially and temporally from MED103 program simulation results of tin plasma produced by Nd:YAG laser. For nanosecond and picosecond laser pulse duration from tin plasma

Pulse Duration	Maximam value: Velocity (cm.sec^{-1})	Time ns	Distance µm
1 ps	1034100	99.5392	1062.9
250 ps	1040300	99.8008	1062.9
500 ps	1030900	99.5032	1039.6
750 ps	1025100	100.003	1031.7
1 ns	11 10^5	23.0066	236.26
10 ns	11 10^6	38.002	3885.3
20 ns	13 10^6	99.000	9545.7
30 ns	12 10^6	100.005	8268.2
40 ns	11 10^6	99.0034	6605.2

2.4 Conclusion

laser pulse duration in a nanosecond at (1 to 40 ns) and nanosecond at (1 to 750 ps) with laser wave intensity of 2.1x1015 w cm-^{2} and λ of 1064 nm was fired at an Sn target; we used the 1-D hydrodynamic MED103 code to study the laser plasma properties and track the Evolution of a few hydrodynamic plasma parameters, the electron density was determined at the first times of the plasma created at the target of pulse duration (1 to 40 ns), the electron temperature seen reaches at the top value of 98 e_V and 25 e_V at 750 ps during,immediately after a laser pulse, the electron density has the maximum at 1024 cm^{-3} and exhibits The pressure begins near the target surface at (1 Mbar), then gradually decreases with changed the distance. The maximum temperature of the ion's 80 eV at a 40 ns laser pulse duration and 20 eV at a laser pulse duration of 750 ps. The maximum value of the ion rate is Z * 21 at 40 ns and Z * 21 at 750 ps. The plasma expansion velocity V_e increases to (12×10^5 cm.sec^{-1}) at 40 ns with plasma distance (7000)µm and velocity V_e =$10*10^5$ cm.sec^{-1}at 750ps with distance remains constant at 1000 µm in a picosecond.

References

[1] A. Mele, A. G. Guidoni, R. Kelly, C. Flamini, and S. J. A. s. s. Orlando, "Laser ablation of metals: Analysis of surface-heating and plume-expansion experiments," vol. 109, pp. 584-590, 1997.

[2] L. Li *et al.*, "Laser nano-manufacturing–state of the art and challenges," vol. 60, no. 2, pp. 735-755, 2011.

[3] G. D. Gautam, A. K. J. O. Pandey, and L. Technology, "Pulsed Nd: YAG laser beam drilling: A review," vol. 100, pp. 183-215, 2018.

[4] I. Zergioti, S. Mailis, N. Vainos, A. Ikiades, C. Grigoropoulos, and C. J. A. S. S. Fotakis, "Microprinting and microetching of diffractive structures using ultrashort laser pulses," vol. 138, pp. 82-86, 1999.

[5] S. Pikuz *et al.*, "Study of SXR/EUV radiation of exploded foils and wires with spectral, spatial and temporal resolution simultaneously on KING electric discharge facility," vol. 30, no. 11, p. 115012, 2021.

[6] R. E. Russo, X. Mao, and S. S. J. A. c. Mao, "The physics of laser ablation in microchemical analysis," vol. 74, no. 3, pp. 70A-77A, 2002.

[7] M. Lenzner, F. Krausz, J. Krüger, and W. J. A. S. S. Kautek, "Photoablation with sub-10 fs laser pulses," vol. 154, pp. 11-16, 2000.

[8] S. Churilov, R. Kildiyarova, A. Ryabtsev, and S. J. P. S. Sadovsky, "EUV spectra of Gd and Tb ions excited in laser-produced and vacuum spark plasmas," vol. 80, no. 4, p. 045303, 2009.

[9] G. Pert and S. J. O. C. Ramsden, "Population inversion in plasmas produced by picosecond laser pulses," vol. 11, no. 3, pp. 270-273, 1974.

[10] T. Higashiguchi *et al.*, "Characteristics of extreme ultraviolet emission from mid-infrared laser-produced rare-earth Gd plasmas," vol. 21, no. 26, pp. 31837-31845, 2013.

[11] C. Suzuki *et al.*, "Extreme ultraviolet spectra from highly charged gadolinium and neodymium ions in the Large Helical Device and laser-produced plasmas," vol. 2013, no. T156, p. 014078, 2013.

[12] A. Cummings, G. O'Sullivan, P. Dunne, E. Sokell, N. Murphy, and J. J. J. o. P. D. A. P. White, "Conversion efficiency of a laser-produced Sn plasma at 13.5 nm, simulated with a one-dimensional hydrodynamic model and treated as a multi-component blackbody," vol. 38, no. 4, p. 604, 2005.

[13] T. Sizyuk and A. J. P. o. P. Hassanein, "Optimizing laser-produced plasmas for efficient extreme ultraviolet and soft X-ray light sources," vol. 21, no. 8, p. 083106, 2014.

[14] J. Christiansen, D. Ashby, and K. J. C. P. C. Roberts, "MEDUSA a one-dimensional laser fusion code," vol. 7, no. 5, pp. 271-287, 1974.

[15] M. S. J. I. J. o. P. Mahmoud, "The emission spectra and hydrodynamic properties of Al plasma using Nd-YAG laser," vol. 16, no. 38, pp. 83-98, 2018.